Mutational analysis of the proteolytic domain of pregnancy-associated plasma protein-A (PAPP-A): classification as a metzincin

Henning B. BOLDT, Michael T. OVERGAARD, Lisbeth S. LAURSEN, Kathrin WEYER, Lars SOTTRUP-JENSEN and Claus OXVIG[1]
Department of Molecular and Structural Biology, University of Aarhus, Science Park, Gustav Wieds Vej 10C, DK-8000 Aarhus C, Denmark

The bioavailability of insulin-like growth factor (IGF)-I and -II is controlled by six IGF-binding proteins (IGFBPs 1–6). Bound IGF is not active, but proteolytic cleavage of the binding protein causes release of IGF. Pregnancy-associated plasma protein-A (PAPP-A) has recently been found to cleave IGFBP-4 in an IGF-dependent manner. To experimentally support the hypothesis that PAPP-A belongs to the metzincin superfamily of metalloproteinases, all containing the elongated zinc-binding motif HEXXHXXGXXH (His-482–His-492 in PAPP-A), we expressed mutants of PAPP-A in mammalian cells. Substitution of Glu-483 with Ala causes a complete loss of activity, defining this motif as part of the active site of PAPP-A. Interestingly, a mutant with Glu-483 replaced by Gln shows residual activity. Known metzincin structures contain a so-called Met-turn, whose strictly conserved Met residue is thought to interact directly with residues of the active site. By further mutagenesis we provide experimental evidence that Met-556 of PAPP-A, 63 residues from the zinc-binding motif, is located in a Met-turn of PAPP-A. Our hypothesis is also supported by secondary-structure prediction, and the ability of a 55-residue deletion mutant (d[S498-Y552]) to express and retain antigenecity. However, because PAPP-A differs in the features defining the individual established metzincin families, we suggest that PAPP-A belongs to a separate family. We also found that PAPP-A can undergo autocleavage, and that autocleaved PAPP-A is inactive. A lack of unifying elements in the sequences around the found cleavage sites of PAPP-A and a variant suggests steric regulation of substrate specificity.

Key words: autocleavage, IGF, insulin-like growth factor-binding protein, metalloproteinase, pappalysin.

INTRODUCTION

Pregnancy-associated plasma protein-A (PAPP-A) was first isolated from human term pregnancy serum in the early 1970s [1]. Although a characteristic metalloproteinase zinc-binding motif was later pointed out in the amino acid sequence of PAPP-A [2,3], its function remained unproven. Only recently was proteolytic activity of PAPP-A demonstrated experimentally [4].

The metzincin superfamily of metalloproteinases is a diverse group of zinc peptidases with members from both the prokaryotes and eukaryotes. It includes four families: the astacins (e.g. crayfish collagenolytic enzyme and bone morphogenetic protein-1), the reprolysins or adamalysins (snake venom proteinases and ADAMs, or a disintegrin and metalloproteinase), the serralysins (bacterial proteinases) and the matrix metalloproteinases (MMPs), also denoted matrixins (vertebrate collagenases) [3]. All metzincins contain the elongated zinc-binding motif, HEXXHXXGXXH, as opposed to the shorter HEXXH motif known from thermolysin and many other zinc peptidases [5], which co-ordinates the catalytic zinc ion of the active site. In addition, as reflected by their common name, they all have a strictly conserved Met residue [6]. Spatially located in close proximity to the zinc ion and its three co-ordinating His residues, this residue is believed to be important for the integrity of the active site.

Three-dimensional structures of several members of each family are known. All metzincin catalytic domains share a common core architecture of five β-strands forming one β-sheet, and three α-helices. The active site lies in a cleft between two half-domains, along the edge of an outer strand of the β-sheet. The overall sequence similarity of the catalytic domains within families is often high, but similarity scores between families are low, typically well below 20 %. Family-specific structural features also distinguish families from one another [3].

PAPP-A was shown recently to cleave the approx. 26 kDa (non-reduced) insulin-like growth factor (IGF)-binding protein (IGFBP)-4 at one site into two halves [4]. IGFBP-4 is one of six homologous proteins, IGFBP-1–6, that bind IGF-I and -II with high affinities [7,8]. Free IGF, but not bound IGF, is bioactive; cleavage of IGFBP-4 causes release of bound IGF. Thus PAPP-A promotes the cellular effects of the IGFs. Interestingly, for reasons unknown, the cleavage of IGFBP-4 by PAPP-A strictly requires the presence of IGF-I or -II [4,9]. Proteolytic activity against IGFBP-4 has been reported from many sources that have also recently been shown to contain PAPP-A. These include conditioned media from human fibroblasts [4], marrow stromal cells [4], osteoblasts [4,10], granulosa cells [11] and vascular smooth-muscle cells [12], in addition to pregnancy serum [13] and ovarian follicular fluid [11]. In all cases polyclonal antibodies against PAPP-A inhibit the cleavage of IGFBP-4. IGFBP-4 is the only reported PAPP-A substrate, and no other enzyme has been claimed to cleave IGFBP-4.

In pregnancy, the 200 kDa PAPP-A monomer of 1547 residues [2] circulates as a disulphide-bound 500 kDa 2:2 complex with the proform of eosinophil major basic protein (proMBP) [14–17]. In this complex, PAPP-A activity against IGFBP-4 is inhibited [13]. Outside pregnancy, PAPP-A exists as a 400 kDa homodimer [4,13]. The IGFBP-4 proteolytic activity of pregnancy serum

Abbreviations used: PAPP-A, pregnancy-associated plasma protein-A; proMBP, proform of eosinophil major basic protein; IGF, insulin-like growth factor; IGFBP, IGF-binding protein; TST, Tris/saline/Tween; MMP, matrix metalloproteinase; LNR, lin-notch motif.

[1] To whom correspondence should be addressed (e-mail co@mbio.aau.dk).

Figure 1 Schematic diagram of the PAPP-A monomer

The PAPP-A monomer of 1547 residues contains two types of sequence motif, three LNRs (LNR1–3, Cys-334–Cys-360, Ala-367–Cys-393 and Cys-1478–Cys-1503), and five short consensus repeats (SCR1–5, Cys-1135–Cys-1200, Cys-1205–Cys-1262, Cys-1266–Cys-1330, Cys-1335–Cys-1391 and Cys-1398–Cys-1474). The localization of the sequence stretch conforming to the metzincin zinc-binding motif (HEXXHXXGXXH, His-482–His-492 in PAPP-A) is indicated by Zn.

most probably stems from a minor fraction of PAPP-A not complexed with proMBP [13].

In addition to the elongated zinc-binding motif, PAPP-A contains three lin-notch motifs (LNR1–3) and five short consensus repeats (SCR1–5) of unknown function [2] (Figure 1). No other protein shares global similarity with PAPP-A, except a recently discovered protein, PAPP-A2, which cleaves IGFBP-5 [18]. PAPP-A2 shares 45 % of its residues with PAPP-A. Residues 147–1791 of PAPP-A2 have also been reported as a putative proteolytic enzyme designated PAPP-E [19].

We sought to establish experimental evidence that PAPP-A belongs to the metzincins, but not to any of the established four families. By mutagenesis and prediction of secondary structure, we define and analyse the proteolytic domain of PAPP-A.

EXPERIMENTAL

Secondary-structure prediction

The secondary structure of the amino acid sequence of PAPP-A was predicted using the set of algorithms included in Jpred2, available online (http://jura.ebi.ac.uk:8888/) [20,21]. The program specifies whether α-helix (h), β-strand (e) or coil structure (−) is the most probable for individual residues. Residues 231–680 were submitted to the server {note that PAPP-A is numbered with the N-terminal Glu of the mature 1547-residue protein as residue 1, and the cDNA sequence is numbered with the codon encoding E1 as nucleotides 1–3, as in [2]; in the deposited sequence record (accession number X68280) this Glu is residue 5 and the corresponding nucleotides are 13–15}. Submission of an alignment with the corresponding sequence of PAPP-A2 [18] resulted in a very similar prediction.

PAPP-A plasmid construction and mutagenesis

A PAPP-A expression plasmid, pcDNA3.1-PAPP-A (pPA), containing cDNA encoding residues 1–1547 of the mature polypeptide cloned into the *Hin*dIII/*Xba*I sites of pcDNA3.1+ (Invitrogen) was made previously [13]. To facilitate mutagenesis, three plasmids containing PAPP-A cDNA corresponding to residues 1–407, 408–988 and 989–1547 were constructed. In brief, using pPA as a template, and two sets of primers [5′-CATTGACGCAAATGGGCGGTAGGC-3′, nucleotides 763–786 of pcDNA3.1+, and 5′-CGCGGA**tCCgGA**TCAAAGCAAGTCTGAGTGAC-3′, corresponding to nucleotides 1226–1201 of PAPP-A, and 5′-CGCGGA**tCCgGA**CTCTCCACACAGAGCCTAC-3′, corresponding to nucleotides 1221–1245 of PAPP-A, and 5′-CAAGCAGCTGCACGCTGATGGTCTC-3′, nucleotides 3130–3106 of PAPP-A], PCR products containing cDNA corresponding to residues 1–407 and 408–988, respectively, were generated using *Pfu* DNA polymerase (Stratagene). Two of the primers contained a *Bam*HI site (underlined) 5′ to the coding sequence. These primers also contained a *Bsp*EI site (in bold), both corresponding to nucleotides 1221–1226 of pPA. The change in the nucleotide sequence, shown by lower-case letters, did not change the encoded amino acid sequence. The two PCR products were digested with *Hin*dIII/*Bam*HI and *Bam*HI/*Kpn*I, respectively, and cloned into pBluescript II SK+ (Stratagene) to generate pB1-407 and pB408-988. To obtain pB989-1547, the *Kpn*I/*Xba*I fragment of pPA was excised and cloned into pBluescript II SK+. Further, the cDNA fragments contained in pB1-407 and pB408-988 were excised with *Hin*dIII/*Bsp*EI and *Bsp*EI/*Kpn*I, respectively, and swapped together into the *Hin*dIII/*Kpn*I sites of pPA, effectively introducing a unique *Bsp*EI site into pPA at the site corresponding to residues 407–408. This variant of pPA is referred to as pPA-BspEI.

Mutagenesis was carried out by QuikChange (Stratagene) using pB408-988 as a template, and the following sets of primers: 5′-CCATGATCCATcAGATTGGTCACAGCCTGG-3′ and 5′-GACCAATCTgATGGATCATGGTGTGGGTG-3′ (for E483Q), 5′-CCATGATCCATGcGATTGGTCACAGCCTGGG-3′ and 5′-GTGACCAATCgCATGGATCATGGTGTGGGTG-3′ (for E483A), 5′-CAACAACTTCtTGAGCTATGCAGATGACGACTG-3′ and 5′-GCATAGCTCAaGAAGTTGTTGTAAGGAGTGTTG-3′ (for M556L), 5′-CTTCATGAGCTtTGCAGATGACGACTGTACGG-3′ and 5′-GTCATCTGCAaAGCTCATGAAGTTGTTGTAAGG-3′ (for Y558F), 5′-CTTCATGAGCgcTGCAGATGACGACTGTACGGAC-3′ and 5′-TCGTCATCTGCAgcGCTCATGAAGTTGTTGTAAGG-3′ (for Y558A), 5′-CCGAGGCATC*AACAACTTCATGAGCTATGCAGATG-3′ and 5′-TGAAGTTGTT*GATGCCTCGGAAGACGTGATAGAGG-3′ (for d[S498-Y552]) and 5′-CAGATGACGACgcTACGGACTCCTTCACGCC-3′ and 5′-GGAGTCCGTAgcGTCGTCATCTGCATAGCTCATG-3′ (for C563A). Mutated residues are shown in lower case, and the sites of deletion are marked with asterisks. The *Bsp*EI/*Kpn*I fragments were excised from the mutated pB408-988 vectors and swapped into the *Bsp*EI/*Kpn*I sites of pPA-BspEI to generate full-length mutated PAPP-A cDNA. Because the introduced *Bsp*EI site is sensitive to methylation, plasmids were propagated in an *Escherichia coli* dam$^-$ strain as needed. All constructs were verified by sequence analysis.

IGFBP-4 plasmid construction

Human placental oligo-dT primed cDNA [22] was used as a template to amplify cDNA encoding human IGFBP-4 (accession number M62403). Specific primers containing an *Xho*I site (5′-TCCGCTCGAGATGCTGCCCCTCTGCCTCGTGGC-3′) and a *Kpn*I site (5′-GACGGTACCCTCTCGAAAGCTGTCAGCCAG-3′) were used (with the sites underlined), and the resulting PCR product was digested and cloned into the *Xho*I/*Kpn*I sites of the expression vector pcDNA3.1/Myc-His(−)A (Invitrogen). The construct pBP4mH encoded the 258-residue proIGFBP-4, followed immediately by residues GTKLGP, the Myc epitope (EQKLISEEDL), residues NSAVD and six His residues. The PCR was carried out with *Pfu* DNA polymerase, and the construct was verified by sequence analysis.

Protein expression and purification

Human embryonic kidney 293T cells (293tsA1609neo) [23] were maintained in high-glucose Dulbecco's modified Eagle's medium supplemented with 10 % fetal bovine serum, 2 mM glutamine, non-essential amino acids and gentamicin (Life Technologies).

Cells were plated on to 6 cm tissue-culture dishes and were transfected 18 h later by calcium phosphate co-precipitation [24] using 10 μg of plasmid DNA prepared by QIAprep Spin Kit (Qiagen). After a further 48 h the supernatants were harvested and cleared by centrifugation, or the cells were first maintained for another 48 h in serum-free medium (293 SFM II, Life Technologies) to facilitate purification (IGFBP-4) or to promote PAPP-A autocleavage.

His-tagged recombinant IGFBP-4 was purified from serum-free medium (20 ml) using a metal-chelate affinity column (2 ml; Pharmacia) charged with nickel ions. Bound protein was eluted with 10 mM EDTA in PBS containing 500 mM NaCl, and further loaded on to a Superdex 75 HR 10/30 column (Pharmacia) equilibrated and eluted with 50 % formic acid to separate any bound IGF. At the acidity of the solvents (pH < 1), any possible bound IGF would dissociate from IGFBP-4 and elute separately. Finally, the eluted IGFBP-4 was loaded directly on to a reversed-phase HPLC column (4 mm × 250 mm Nucleosil C_4 500-7; Macherey-Nagel, Düren, Germany) eluted at a flow rate of 0.5 ml/min. A linear gradient was formed from 0.1 % (v/v) trifluoroacetic acid (solvent A) and 0.075 % (v/v) trifluoroacetic acid in 90 % (v/v) acetonitrile (solvent B), increasing the amount of solvent B by 2.3 %/min. The column was equilibrated with 5 % solvent B, operated at 50 °C, and the separation was monitored at 226 nm. IGFBP-4 eluted at about 42 % solvent B. This latter step alone was not sufficient, as IGF (Bachem) co-eluted with IGFBP-4 on this column, as seen in separate runs. The material was lyophilized, redissolved in solvent A, and further diluted three times in 50 mM Tris/HCl, pH 7.5.

Measurement of PAPP-A proteolytic activity

Purified IGFBP-4 (1 μg) was ^{125}I-labelled [25], and IGFBP-4 proteolytic activity was measured using approx. 40000 c.p.m. (approx. 3 ng) [^{125}I]IGFBP-4 contained in 250 mM sodium phosphate, pH 8.0 (2 μl). The reaction mixture further contained 0.3 ng of PAPP-A (1 μl of PAPP-A containing standard serum medium diluted approx. 25 times in 50 mM Tris/HCl, pH 7.5 to contain 0.3 ng of PAPP-A/μl), 20 nM IGF-II (Bachem) diluted from a stock solution of 20 μM in 1 mM HCl (1 μl) and 50 mM Tris/HCl, pH 7.5, to a final volume of 20 μl. After incubation at 37 °C (2–72 h, as specified), the reaction was stopped by addition of 10 mM EDTA, and the mixture was separated by non-reducing SDS/PAGE (16 % gel) [26]. For comparison of PAPP-A mutants with wild-type PAPP-A, conditions were chosen (2 h of incubation) that resulted in about 70 % degradation of IGFBP-4 by wild-type PAPP-A. The degree of cleavage was determined by quantification of band intensities using a PhosphoImager (Molecular Dynamics). After subtraction of background signal (< 5 %), activities were expressed as the percentage of IGFBP-4 degradation compared with that of wild-type PAPP-A (set to 100 %). For measurement of the effect on activity of PAPP-A autocleavage, the activities of PAPP-A expressed in serum medium (< 5 % autocleavage) and serum-free medium (> 90 % autocleavage) were compared. Prior to assay, to provide identical contexts, an equal volume of serum-free medium from mock transfectants was added to the PAPP-A contained in serum medium, and vice versa.

Miscellaneous procedures

SDS/PAGE was performed in Tris/glycine gels (10–20 % or 16 %) [26]. Separated proteins were visualized by Western blotting or by staining with Coomassie Brilliant Blue. For immunovisualization, blots were blocked with 2 % Tween 20 and equilibrated in 50 mM Tris/HCl/500 mM NaCl/0.1 % Tween 20, pH 9.0 (Tris/saline/Tween, TST). Monoclonal antibody [27] (mAb 234-2, for detection of unreduced PAPP-A) or polyclonal antibodies [28] (for detection of reduced or unreduced PAPP-A) were used. The antibodies were diluted in TST containing 0.5 % fetal bovine serum, and blots were incubated for 1 h at 37 °C. Incubation with peroxidase-conjugated secondary antibodies (P260 or P217, Dako) diluted in TST was done for 1 h at room temperature. Blots were developed using enhanced chemiluminescence (ECL, Amersham). The levels of recombinant PAPP-A in the supernatants were measured by a standard sandwich ELISA as described previously [13]. For sequence analysis of PAPP-A fragments generated by autocleavage, antigen was affinity-purified on anti-PAPP-A/proMPB [28] immobilized on CNBr-activated Sepharose (Pharmacia) according to the manufacturer's protocol. Bound protein was eluted with 200 mM glycine, pH 2.2, separated on 10–20 % reducing SDS/PAGE, blotted on to a PVDF membrane and stained with Coomassie Brilliant Blue. Bands were excised, and sequence analysis was performed on an Applied Biosystems 477A sequencer equipped with an online HPLC [29] at levels of approx. 20 pmol.

RESULTS AND DISCUSSION

The putative zinc-binding site of PAPP-A forms its active site

Based on the presence of the elongated zinc-binding motif, it had been speculated previously that PAPP-A possesses proteolytic activity [2], but experimental evidence for this was only presented recently [4]. It was shown that media conditioned by human fibroblasts contained PAPP-A and degraded IGFBP-4. Interestingly, this occurred only in the presence of IGF-I or -II. However, PAPP-A might be physically associated with an unidentified proteinase, which in turn is the enzyme responsible for cleavage of IGFBP-4, or PAPP-A might function to activate an unknown proteinase by binding to it. To exclude this, we first constructed two variants of PAPP-A mutated in the zinc-binding motif by site-directed mutagenesis.

The strictly conserved Glu immediately following the first His in the zinc-binding motif (Glu-483 in PAPP-A) is thought to polarize (deprotonate) a zinc-bound water molecule that attacks

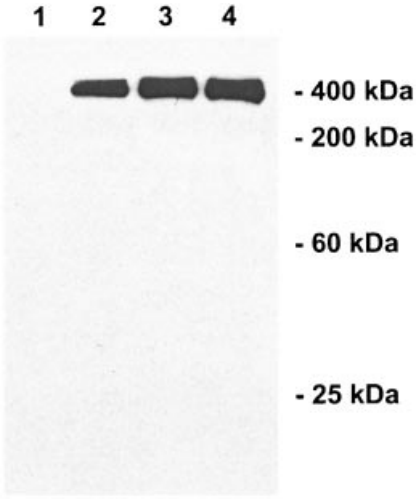

Figure 2 Western blot of wild-type PAPP-A and its Glu-483 mutants

Western blot using polyclonal antibodies of serum-free medium from cells transfected with empty vector (lane 1), vector containing cDNA encoding mature, wild-type PAPP-A (lane 2), mutant E483Q (lane 3) or mutant E483A (lane 4). All samples were non-reduced.

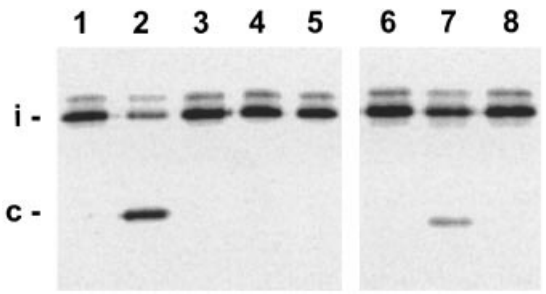

Figure 3 Activity of PAPP-A with Glu-483 replaced by Gln or Ala

Wild-type PAPP-A (0.3 ng) was incubated (4 h) with radiolabelled IGFBP-4 in the presence (lane 2) and absence (lane 3) of IGF-II, showing the dependence of IGF. Under these conditions, in the presence of IGF, mutants E483Q (lane 4) and E483A (lane 5) did not show activity. Incubation with medium from cells transfected with empty vector is shown in lane 1. Longer incubation (48 h) using more mutated enzyme (2 ng) revealed residual activity of mutant E483Q (lane 7), but no activity of E483A (lane 8) or medium from cells transfected with empty vector (lane 6). Intact (i) IGFBP-4 and its cleavage fragments (c) are indicated. Co-migration of the N-terminal and the C-terminal cleavage products is caused by the C-terminal tag of IGFBP-4. The less intense of the two upper uncleaved bands is glycosylated IGFBP-4.

Proteinase	Zinc binding motif	Gap	Met-turn
Astacins			
Astacin	HELMHAIGFYH**E**	-44-	**S**IMHY
BMP1	HELGHVVGFWH**E**	-46-	**S**IMHY
Reprolysins			
Adamalysin II	HELGHNLGMEH**D**	-13-	**C**IMRP
ADAM 12	HELGHNFGMNH**D**	-19-	**C**IMNA
Serralysins			
Alk.proteinase	HEIGHTLGLSH**P**	-27-	**S**VMSY
Serralysin	HEIGHALGLSH**P**	-27-	**S**LMSY
Matrix metalloproteinases (MMPs)			
Collagenase n	HEFGHSLGLAH**S**	-7-	**A**LMYP
Matrilysin	HELGHSLGMGH**S**	-7-	**A**VMYP
Pappalysins			
PAPP-A	HEIGHSLGLYH**V**	-63-	**N**FMSY
PAPP-A2	HEVGHVLGLYH**V**	-63-	**N**YMSY

Figure 4 Residues of zinc-binding site and Met-turn of metzincin families

Sequences from two representative members of each of the four established metzincin families are aligned. The gap is the number of residues between the third His residue (H) of the zinc-binding consensus sequence and the Met residue (M) of the Met-turn. Residues strictly conserved within the metzincin superfamily are underlined. Conserved residues within each family are shown in bold [3]. Sequences were taken from [3], except that of ADAM 12 (a disintegrin and metalloproteinase 12) [44]. The corresponding zinc-binding sequence and the putative Met-turn sequence of PAPP-A [2] and PAPP-A2 [18] are also shown. With PAPP-A2, PAPP-A defines a fifth family, which we suggest to be named the pappalysins. BMP1, bone morphogenetic protein-1.

the peptide bond to be cleaved, as suggested for astacin [30]. Thus variants of the PAPP-A cDNA were made, encoding mutants E483Q and E483A. When expressed in mammalian cells [13], both mutants were secreted at wild-type levels at least, as measured by ELISA using six different available PAPP-A monoclonal antibodies that do not recognize reduced and denatured PAPP-A [27] (results not shown), and they migrated in SDS/PAGE like wild-type PAPP-A (Figure 2).

No low-molecular-mass substrate is available for PAPP-A; IGFBP-4 is the only known PAPP-A substrate. Therefore, to measure activity of wild-type PAPP-A and PAPP-A mutants, we used a gel-based assay. Human IGFBP-4 cDNA was cloned, expressed in mammalian cells, purified and ^{125}I-labelled. The radiolabelled IGFBP-4 was incubated with PAPP-A or PAPP-A mutants, and activity was assessed by separation of intact IGFBP-4 and its cleavage products in SDS/PAGE followed by autoradiography (Figure 3). As expected, wild-type PAPP-A degraded IGFBP-4 in the presence of IGF, but not in its absence (Figure 3, lanes 2 and 3). Both E483Q and E483A showed a complete loss of activity against IGFBP-4 under conditions where about 90% of the substrate was degraded by the same amount of wild-type PAPP-A (Figure 3, lanes 4 and 5). Extended incubation using more enzyme, however, showed residual activity of E483Q, but not E483A (Figure 3, lanes 7 and 8). With this experiment, we establish the basis for the metalloproteolytic activity of PAPP-A by demonstrating that the putative zinc-binding site of PAPP-A participates in formation of the active site.

Although it is generally accepted, and supported by numerous studies on similar enzymes [31–34], the concept that the conserved Glu in enzymes with either of the two zinc-binding motifs functions as a general base catalyst in substrate hydrolysis has been contradicted [35–37]. Thus residues outside the zinc-binding motif have been proposed to play the role of the general base. Our results do not allow discrimination between those views, but do show that Glu-483 is critical for efficient substrate hydrolysis.

Hypothesis: PAPP-A belongs to the metzincin superfamily of metalloproteinases

The above experiment showed that PAPP-A is the enzyme directly responsible for cleavage of IGFBP-4, and that the elongated zinc-binding motif participates in formation of its active site. We hypothesized further that PAPP-A belongs to the metzincin superfamily of metalloproteinases, also comprising the structurally conserved Met-turn, as well as a conserved overall topology [6]. Interestingly, the family-specific residue immediately following the third His residue of the zinc-binding motif is a Val in PAPP-A, different from any of the known families [38] (Figure 4).

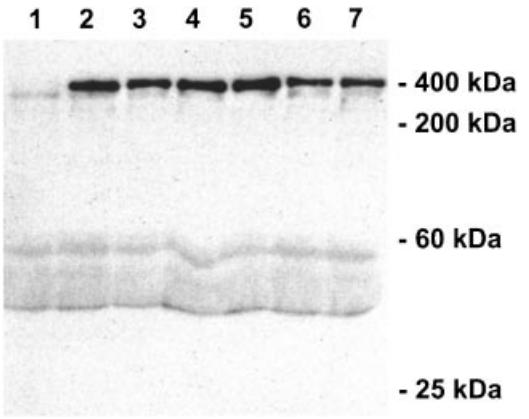

Figure 5 Verification of expression of PAPP-A mutants

Western blot using a PAPP-A monoclonal antibody of standard medium from cells transfected with empty vector (lane 1), vector containing cDNA encoding wild-type PAPP-A (lane 2), mutant M556L (lane 3), mutant Y558F (lane 4), mutant Y558A (lane 5), mutant C563A (lane 6) or mutant d[S498-Y552] (lane 7). All samples were non-reduced.

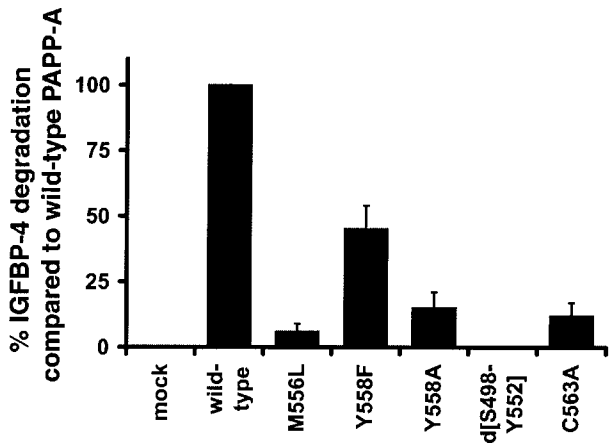

Figure 6 Ability of PAPP-A mutants to cleave IGFBP-4 compared with wild-type PAPP-A

The degree of cleavage of radiolabelled IGFBP-4 was determined by quantification of band intensities. Conditions were chosen (2 h of incubation) that resulted in about 70% degradation of IGFBP-4 by wild-type PAPP-A. Activities are expressed as the percentage of IGFBP-4 degradation compared with wild-type PAPP-A (set to 100%). Values are mean ± S.D. ($n = 3$). Mutated variants of PAPP-A were used in the same amounts as wild-type PAPP-A, as measured by ELISA. For this assay, all constructs were expressed in serum-containing medium.

Some residues of the sequence that are close in the primary structure to the conserved Met residue show limited variation within each of the four metzincin families, as does the number of residues between the zinc-binding motif and the Met residue (Figure 4). In PAPP-A, three candidate Met-turn residues, Met-508, Met-556 and Met-575, are present within the first 150 residues following the zinc-binding motif (His-482–His-492). Only Met-556 has a hydrophobic residue on its N-terminal side, a characteristic feature of all metzincins. Further, the two residues following Met-556 (Ser-Tyr) are also found in the serralysins (Figure 4). Although an Asn residue is never found two residues before the Met of the Met-turn in known metcinzins (Figure 4), and, although it implies that the linear distance to the zinc-binding motif is unusually long (Figure 4), we hypothesized that Met-556 of PAPP-A is a Met-turn residue.

To support this experimentally, Met-556 was substituted with Leu, and Tyr-558 with Phe and Ala. The three mutants, M556L, Y558F and Y558A, were expressed at levels similar to wild-type PAPP-A as evaluated by ELISA (results not shown) and Western blotting (Figure 5), and they were all capable of specific proteolysis of IGFBP-4 at one site. However, their activities differed greatly (Figure 6). The Met residue is generally believed to provide structural integrity to the active site. Based on solved metzincin structures, the sulphur atom of the Met may interact directly with the zinc, or its ϵ-methyl group may interact with all three zinc-binding His residues [39]. In accordance with this, we observed a dramatic reduction (93%) in the activity of M556L compared with wild-type PAPP-A (Figure 6), demonstrating the importance of this residue. This points strongly to Met-556 as a Met-turn residue of PAPP-A. In known structures, the Met residue is located underneath the cavity formed by the zinc-binding His residues. Interestingly, our finding that PAPP-A does have enzymic activity with Leu in its place suggests that the Met residue also functions by providing hydrophobicity and, in turn, enhanced zinc binding by the His residues.

The hydroxy group of Tyr in the Met-turn of astacins and serralysins participates in zinc co-ordination in the absence of bound substrate. Substrate binding causes the Tyr residue to rotate, and it probably functions in transition-state stabilization [30]. Substitution of Tyr-558 of PAPP-A with Phe (Y558F) results in a substantial (55%) reduction of activity. When replaced with Ala (Y558A), most (85%) of the activity is lost (Figure 6). This supports an analogous role of co-ordination and stabilization for this residue in PAPP-A. However, its role may be more critical in other metzincins; substitution with Ala in astacin was reported recently to cause an almost complete (97.5%) loss of activity [40].

To support our hypothesis further, we deleted 55 of the 63 residues between the zinc-binding motif and Met-556 (Figure 4). If PAPP-A has the general fold of a metzincin, a major deletion in this stretch might be allowed without disruption of the overall domain structure. Indeed, as judged by ELISA using six monoclonal antibodies as above (results not shown) and Western blotting (Figure 5), the mutated protein, d[S498-Y552], folded and expressed as the wild-type protein. It did not retain the ability to cleave IGFBP-4 (Figure 6), pointing at the deleted region as important in binding of substrate, or for proper organization of the active site. It will be very interesting to compare this mutant with wild-type PAPP-A when a small peptide substrate becomes available.

Prediction and interpretation of PAPP-A secondary structure

To globally evaluate our hypothesis, we asked whether the prediction of secondary structure using Jpred [20,21] supported the hypothesis that PAPP-A is a metzincin. The structural elements common to all metzincins, five β-strands (S1–S5) and three α-helices (HA–HC), were distributed according to the predicted secondary structure in the common order of their occurrence [3] (Figure 7). First it was assumed that residues of the zinc-binding motif formed HB, ending at Gly-489. Although not supported by the prediction, this is a reasonable assumption based on all known metzincin structures. Secondly, in addition to β-strand prediction, the localization of S1 was supported by local similarity in sequence (groups of two or three residues in otherwise non-homologous proteins) between PAPP-A and S1 of known metzincins (Figure 7). Within this frame, the remaining secondary-structural elements were positioned according to the prediction (Figure 7). The prediction of a long helix for residues Gln-571–Tyr-583 (HC), combined with the absence of predicted secondary-structural elements in the sequence stretch from the C-terminus of the zinc-binding motif (His-482) to residue Gln-571, further support Met-556 as a Met-turn residue.

Three α-helices (H-i, H-ii and H-iii) were predicted to be inserted between S2 and S3, S3 and S4, and S4 and S5, respectively (Figure 7). Helices after S3 (H-ii) and S4 (H-iii) have not been observed in known metzincins, which in general have far fewer residues between these strands. In contrast, the predicted presence in PAPP-A of an α-helix after S2 (H-i) is in accordance with the known secondary structure of the reprolysins (Figure 8).

Astacins, serralysins and MMPs have a strictly conserved Trp situated about two (in astacins and MMPs) or about nine (in serralysins) residues before the beginning of the first β-strand, S1. Furthermore, in known three-dimensional structures of these proteins, residues preceding this Trp run parallel to the last α-helix, HC, attached through a salt bridge to a conserved Asp residue of this helix (MMPs and serralysins), or to the conserved Glu next to the third zinc histidine ligand of astacins. The reprolysins, in contrast, do not have this conserved Trp, and solved structures show that, in this family, residues preceeding S1 are not attached to helix HC. No Trp is present in the

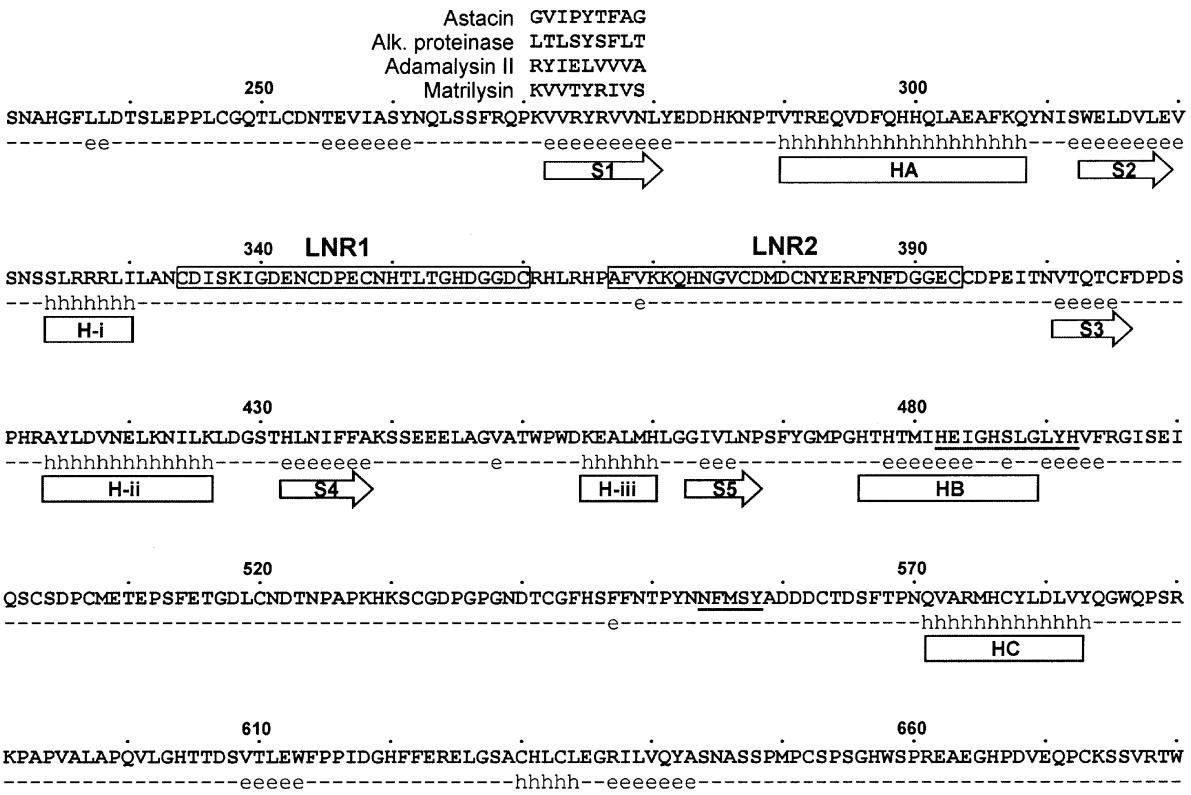

Figure 7 Predicted secondary structure of PAPP-A

Secondary structure within the amino acid sequence of PAPP-A was predicted using Jpred2. Prediction of either α-helix (h), β-strand (e) or coil structure (—) is shown below individual residues. Based on this prediction, secondary-structure elements S1–S5 and HA–HC, found in all known metzincin structures [3], are positioned within the sequence of PAPP-A. The shown lengths (in number of residues) of S1–S5 and HA–HC are as found in the known structures (S1, 9; S2, 7; S3, 6; S4, 7; S5, 6; HA, 19; HB, 14; HC, 12). Importantly, the position of S1 is supported further by local similarities between PAPP-A and known metzincins, illustrated by alignment of selected S1 sequences [3]. In the position of HB, no helix prediction was found. However, an α-helix ending at the conserved glycine in the zinc-binding motif is invariably present in known structures with this motif. It is predicted that in addition to those elements, three helices are present in the proteolytic domain of PAPP-A, H-i, H-ii and H-iii, also shown by rectangles. The reprolysins have a helix corresponding to H-i, but H-ii and H-iii are unique to PAPP-A (see Figure 8). The zinc-binding motif and predicted Met-turn residues are underlined, and residues of LNR1 and LNR2 are boxed. Numbering is according to [2].

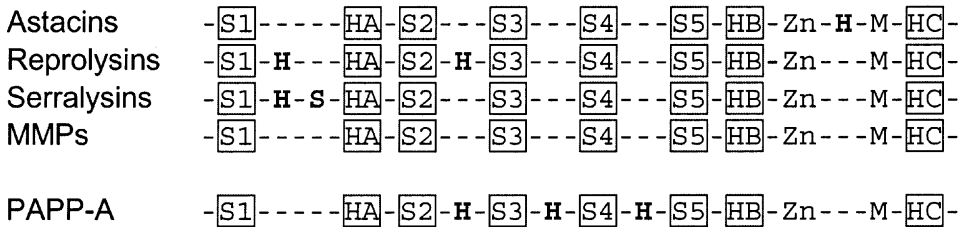

Figure 8 Secondary structure within the metzincin superfamily

The experimentally determined secondary structure, characteristic of the proteolytic domain of each metzincin family member, is shown for the astacins, reprolysins, serralysins and MMPs [3]. The predicted secondary structure of PAPP-A (see Figure 7) is also shown. Boxed elements (strands S1–S5 and helices HA–HC) are present in all superfamily members. Elements shown in bold are family-specific. The positions of the zinc-binding motif (Zn) and the Met-turn (M) are indicated.

corresponding position of PAPP-A; the closest Trp is separated by 54 residues from the predicted S1. Whether the residues before the predicted S1 in PAPP-A run parallel to HC is unknown, but the presence of a long-range disulphide bond between Cys-252 (preceeding the predicted S1) and Cys-577 (within the predicted HC) unequivocally demonstrates that these residues, separated by 324 residues in the sequence, are in close proximity in the three-dimensional structure of PAPP-A (M. T. Overgaard, L. Sottrup-Jensen and C. Oxvig, unpublished work; the PAPP-A monomer contains a total of 82 Cys residues whose pairing within the heterotetrameric PAPP-A/proMBP complex are currently being elucidated by analysis of derived peptides; the knowledge of a disulphide bond between Cys-252 and Cys-577 is a partial result of this ongoing investigation). This disulphide bond is likely to be comparable with the mentioned salt bridges.

Taken together, several lines of evidence suggest that PAPP-A belongs to the metzincin superfamily of metalloproteinases.

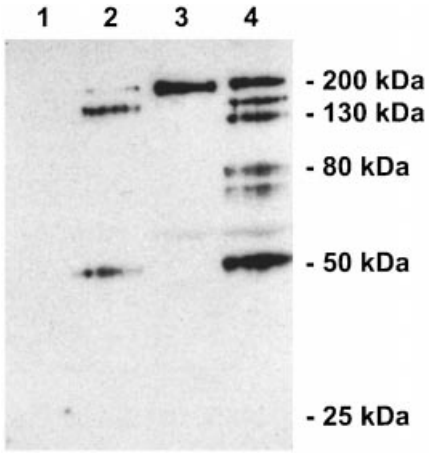

Figure 9 Autocleavage of PAPP-A and PAPP-A mutant C563A

Western blot using polyclonal antibodies of serum-free medium from cells transfected with empty vector (lane 1), vector containing cDNA encoding wild-type PAPP-A (lane 2), mutant E483A (lane 3) and mutant C563A (lane 4). All samples were reduced. Faint non-specific staining is seen just above the 50 kDa band.

PAPP-A, autocleavage:
(377) CDMDCNYERF|NFDGGECCDP (396)

PAPP-A C563A, autocleavage:
(358) GDCRHLRHPA|FVKKQHNGVC (377)
(977) DLSEGISQHA|WYPCTISYPY (996)

PAPP-A cleavage of IGFBP-4:
(126) RDRSTSGGKM|KVNGAPREDA (145)

Figure 10 Alignment of residues surrounding PAPP-A autocleavage sites

The major autocleavage site of PAPP-A and the two major autocleavage sites of mutant C563A are indicated by vertical bars in the sequence of PAPP-A. The cleavage sites were determined by sequence analysis of proteolytic fragments separated by reducing SDS/PAGE and blotted on to a PVDF membrane. For comparison, the published [41] PAPP-A cleavage site of IGFBP-4 is also shown.

However, as PAPP-A cannot be classified with any of the four recognized families, we propose the existence of a fifth family, the *pappalysins*. The arguments used above are also supported by analysis of the sequence of PAPP-A2 (results not shown).

Autocleavage of PAPP-A

By SDS/PAGE of reduced rPAPP-A or PAPP-A/proMBP purified from pregnancy serum, very limited ($< 5\%$) but apparently specific proteolysis of PAPP-A has previously been observed [13–15]. The cleavage was thought to be caused by other proteinases present in the serum and/or secreted from the cells transfected with PAPP-A cDNA. While limited in standard serum-containing medium, culture of wild-type PAPP-A transfectants in serum-free medium caused pronounced cleavage, dependent on the length of incubation. Apparently, standard serum-containing medium protected PAPP-A from cleavage. Interestingly, Western blotting (using polyclonal antibodies) of reduced PAPP-A mutated at Glu-483 did not show any fragmentation, demonstrating it to be caused by autoproteolytic activity of the wild-type protein, not by unknown proteinase(s) (Figure 9, lanes 2 and 3).

In addition to the intact PAPP-A monomer of 200 kDa, two bands of about 150 kDa and 50 kDa were seen in the reducing Western blot (Figure 9, lane 2). By Edman degradation of purified protein separated by reducing SDS/PAGE and blotted on to a PVDF membrane, the 50 kDa band was identified as the PAPP-A N-terminal fragment. The N-terminus of the 150 kDa band (NFDGGE …) revealed that autocleavage occurred between Phe-386 and Asn-387, located at the C-terminal end of LNR2 within the proteolytic domain (Figure 10). This is interesting because, other than IGFBP-4, no substrate has been found that can be cleaved by PAPP-A. The found site shows similarities with, but also marked differences from, the reported cleavage site in IGFBP-4 (Figure 10) [41,42].

Relative to the organization of the common metzincin secondary-structural elements, the prototype active site is widely exposed to solvent [3]. However, flexible loop structures may partially cover this face of the domain, and govern access to the active site. The presence of a Cys residue between the Met-turn and α-helix HC is a unique feature of PAPP-A (Cys-563). Although it is currently not known whether or how Cys-563, six residues after the Met-turn Met, engages in disulphide pairing, we speculated that this residue might dictate restricted access to the active site by imposing the conformational restraints of a disulphide bond to the sequence stretch between the Met-turn and helix HC.

Indeed, the C563A mutated protein showed a cleavage pattern different from that of the wild-type (Figure 9). Further, the autocleavage of C563A was more pronounced, and occurred in serum-containing medium to a greater extent than wild-type PAPP-A. Thus Edman degradation was performed as with the wild-type protein. The N-terminal sequence of the approx. 150 kDa band (FVKKQH …) surprisingly revealed autocleavage between Ala-367 and Phe-368. This site is also within LNR2 of the proteolytic domain, but 19 residues N-terminal to the one wild-type autocleavage site. The sequence of the band at about 70 kDa (WYPCTI …) showed that cleavage between Ala-986 and Trp-987 also occurred. This site is separated by 400 residues from the proteolytic domain. In accordance with the estimated molecular masses, the third band from the top (130 kDa) is the N-terminal fragment resulting from cleavage after Ala-986 only; this fragment (containing the still-intact proteolytic domain) is most likely further partially processed into the 80 kDa band (FVKKQH …) just above the 70 kDa band plus the lower 50 kDa band (N-terminal fragment). Thus the lack of unifying elements in the sequences around the found cleavage sites of PAPP-A (Figure 10) implies that the specificity of PAPP-A is determined by steric restrictions more than required interactions between PAPP-A and specific substrate side chains.

We finally asked whether PAPP-A autocleavage affected the ability of PAPP-A to cleave IGFBP-4 by comparing the activities of wild-type PAPP-A expressed in standard serum-containing medium (SE-PAPP-A, $< 5\%$ autocleavage) and PAPP-A expressed in serum-free medium (SFM-PAPP-A, $> 90\%$ autocleavage). Precise comparison is difficult because the amount of intact PAPP-A cannot be estimated accurately. However, we found that almost 30-fold more SFM-PAPP-A than SE-PAPP-A was required to obtain the same degree (approx. 50%) of degradation (results not shown). This is compatible with a complete loss of activity following autocleavage, but a residual activity of autocleaved PAPP-A cannot be excluded. Autolytic cleavage is known from other metzincins, for example MMP-2, in which the proteolytic activity is also lost [43]. When compared with wild-type PAPP-A, mutant C563A showed a large decrease

in activity against IGFBP-4 (Figure 6). As mentioned, unlike wild-type PAPP-A, C563A showed pronounced autocleavage when cultured in serum medium; the decrease in activity most likely reflects a difference in the extent of autocleavage. However, the mutation itself may also directly affect the cleavage of IGFBP-4.

Although autocleavage of PAPP-A does occur *in vivo*, these experiments do not address its potential relevance. However, it shows the importance of considering the extent of autolytic cleavage whenever PAPP-A synthesized by cells grown in serum-free media is used for experiments *in vitro*.

Conclusions

We have established that Glu-483 is critical for the catalytic activity of PAPP-A. Substitution with Ala abolished PAPP-A activity towards IGFBP-4. PAPP-A with Glu-483 replaced by Gln, however, showed residual activity. Using mutagenesis we have also identified a Met-turn in the sequence of PAPP-A. Thus PAPP-A belongs to the large metzincin family of metalloproteinases. Predicted secondary structure, local sequence similarities of PAPP-A with known metzincin sequences and a known long-range disulphide bond also support this interpretation. Further, a mutant carrying a 55-residue deletion of a predicted loop can be expressed and is antigenic.

According to the pattern of conservation around the Met-turn, PAPP-A resembles proteins of the serralysin family (MSY). The presence of a Tyr residue two residues after the Met is also shared with the astacins. Further, the absence of the strictly conserved Trp residue before β-strand S1 is shared with the reprolysins. However, unlike any of the recognized metzincin families, PAPP-A has a hydrophobic residue (Val) immediately following the third His of the zinc-binding motif. Based on these findings, on the unusual long distance between the zinc-binding motif and the Met-turn, and on the additional secondary-structural elements predicted for PAPP-A, we believe that PAPP-A should be considered as the first member of a new metzincin family, the pappalysins. PAPP-A2 [18], matching the same criteria, is thus the second member of this family.

This work was supported by grants from the Danish Medical Research Council, the Novo Nordic Foundation and the Alfred Benzon Foundation.

REFERENCES

1 Lin, T. M., Galbert, S. P., Kiefer, D., Spellacy, W. N. and Gall, S. (1974) Characterization of four human pregnancy-associated plasma proteins. Am. J. Obstet. Gynecol. **118**, 223–236

2 Kristensen, T., Oxvig, C., Sand, O., Møller, N. P. and Sottrup-Jensen, L. (1994) Amino acid sequence of human pregnancy-associated plasma protein-A derived from cloned cDNA. Biochemistry **33**, 1592–1598

3 Stöcker, W., Grams, F., Baumann, U., Reinemer, P., Gomis-Rüth, F. X., McKay, D. B. and Bode, W. (1995) The metzincins–topological and sequential relations between the astacins, adamalysins, serralysins, and matrixins (collagenases) define a superfamily of zinc-peptidases. Protein Sci. **4**, 823–840

4 Lawrence, J. B., Oxvig, C., Overgaard, M. T., Sottrup-Jensen, L., Gleich, G. J., Hays, L. G., Yates 3rd, J. R. and Conover, C. A. (1999) The insulin-like growth factor (IGF)-dependent IGF binding protein-4 protease secreted by human fibroblasts is pregnancy-associated plasma protein-A. Proc. Natl. Acad. Sci. U.S.A. **96**, 3149–3153

5 Vallee, B. L. and Auld, D. S. (1990) Zinc coordination, function, and structure of zinc enzymes and other proteins. Biochemistry **29**, 5647–5659

6 Bode, W., Gomis-Rüth, F. X. and Stöckler, W. (1993) Astacins, serralysins, snake venom and matrix metalloproteinases exhibit identical zinc-binding environments (HEXXHXXGXXH and Met-turn) and topologies and should be grouped into a common family, the 'metzincins'. FEBS Lett. **331**, 134–140

7 Jones, J. I. and Clemmons, D. R. (1995) Insulin-like growth factors and their binding proteins: biological actions. Endocr. Rev. **16**, 3–34

8 Hwa, V., Oh, Y. and Rosenfeld, R. G. (1999) The insulin-like growth factor-binding protein (IGFBP) superfamily. Endocr. Rev. **20**, 761–787

9 Conover, C. A., Kiefer, M. C. and Zapf, J. (1993) Posttranslational regulation of insulin-like growth factor binding protein-4 in normal and transformed human fibroblasts. Insulin-like growth factor dependence and biological studies. J. Clin. Invest. **91**, 1129–1137

10 Qin, X., Byun, D., Lau, K. W., Baylink, D. J. and Mohan, S. (2000) Evidence that the interaction between insulin-like growth factor (IGF)-II and IGF binding protein (IGFBP)-4 is essential for the action of the IGF-II-dependent IGFBP-4 protease. Arch. Biochem. Biophys. **379**, 209–216

11 Conover, C. A., Oxvig, C., Overgaard, M. T., Christiansen, M. and Giudice, L. C. (1999) Evidence that the insulin-like growth factor binding protein-4 protease in human ovarian follicular fluid is pregnancy associated plasma protein-A. J. Clin. Endocrinol. Metab. **84**, 4742–4745

12 Bayes-Genis, A., Schwartz, R. S., Lewis, D. A., Overgaard, M. T., Christiansen, M., Oxvig, C., Ashai, K., Holmes, D. R. and Conover, C. A. (2001) Insulin-like growth factor binding protein-4 protease produced by smooth muscle cells increases in the coronary artery after angioplasty. Arterioscler. Thromb. Vasc. Biol. **21**, 335–341

13 Overgaard, M. T., Haaning, J., Boldt, H. B., Olsen, I. M., Laursen, L. S., Christiansen, M., Gleich, G. J., Sottrup-Jensen, L., Conover, C. A. and Oxvig, C. (2000) Expression of recombinant human pregnancy-associated plasma protein-A and identification of the proform of eosinophil major basic protein as its physiological inhibitor. J. Biol. Chem. **275**, 31128–31133

14 Oxvig, C., Sand, O., Kristensen, T., Gleich, G. J. and Sottrup-Jensen, L. (1993) Circulating human pregnancy-associated plasma protein-A is disulfide-bridged to the proform of eosinophil major basic protein. J. Biol. Chem. **268**, 12243–12246

15 Oxvig, C., Sand, O., Kristensen, T., Kristensen, L. and Sottrup-Jensen, L. (1994) Isolation and characterization of circulating complex between human pregnancy-associated plasma protein-A and proform of eosinophil major basic protein. Biochim. Biophys. Acta **1201**, 415–423

16 Bonno, M., Oxvig, C., Kephart, G. M., Wagner, J. M., Kristensen, T., Sottrup-Jensen, L. and Gleich, G. J. (1994) Localization of pregnancy-associated plasma protein-A and colocalization of pregnancy-associated plasma protein-A messenger ribonucleic acid and eosinophil granule major basic protein messenger ribonucleic acid in placenta. Lab. Invest. **71**, 560–566

17 Popken-Harris, P., Thomas, L., Oxvig, C., Sottrup-Jensen, L., Kubo, H., Klein, J. S. and Gleich, G. J. (1994) Biochemical properties, activities, and presence in biologic fluids of eosinophil granule major basic protein. J. Allergy Clin. Immunol. **94**, 1282–1289

18 Overgaard, M. T., Boldt, H. B., Laursen, L. S., Sottrup-Jensen, L., Conover, C. A. and Oxvig, C. (2001) Pregnancy-associated plasma protein-A2 (PAPP-A2) a novel insulin-like growth factor binding protein-5 proteinase. J. Biol. Chem. **276**, 21849–21853

19 Farr, M., Strube, J., Geppert, H., Kocourek, A., Mahne, M. and Tschesche, H. (2000) Pregnancy-associated plasma protein-E (PAPP-E). Biochim. Biophys. Acta **1493**, 356–362

20 Cuff, J. A. and Barton, G. J. (1999) Evaluation and improvement of multiple sequence methods for protein secondary structure prediction. Proteins **34**, 508–519

21 Cuff, J. A. and Barton, G. J. (2000) Application of multiple sequence alignment profiles to improve protein secondary structure prediction. Proteins **40**, 502–511

22 Overgaard, M. T., Oxvig, C., Christiansen, M., Lawrence, J. B., Conover, C. A., Gleich, G. J., Sottrup-Jensen, L. and Haaning, J. (1999) Messenger ribonucleic acid levels of pregnancy-associated plasma protein-A and the proform of eosinophil major basic protein: expression in human reproductive and nonreproductive tissues. Biol. Reprod. **61**, 1083–1089

23 DuBridge, R. B., Tang, P., Hsia, H. C., Leong, P. M., Miller, J. H. and Calos, M. P. (1987) Analysis of mutation in human cells by using an Epstein-Barr virus shuttle system. Mol. Cell. Biol. **7**, 379–387

24 Pear, W. S., Nolan, G. P., Scott, M. L. and Baltimore, D. (1993) Production of high-titer helper-free retroviruses by transient transfection. Proc. Natl. Acad. Sci. U.S.A. **90**, 8392–8396

25 Greenwood, F. C., Hunter, W. M. and Glover, J. S. (1963) The preparation of ^{131}I-labelled human growth hormone of high specific radioactivity. Biochem. J. **89**, 114–123

26 Laemmli, U.K. (1970) Cleavage of structural proteins during the assembly of the head of bacteriophage T4. Nature (London) **227**, 680–685

27 Qin, Q. P., Christiansen, M., Oxvig, C., Pettersson, K., Sottrup-Jensen, L., Koch, C. and Norgaard-Pedersen, B. (1997) Double-monoclonal immunofluorometric assays for pregnancy-associated plasma protein A/proeosinophil major basic protein (PAPP-A/proMBP) complex in first-trimester maternal serum screening for Down syndrome. Clin. Chem. **43**, 2323–2332

28 Christiansen, M., Oxvig, C., Wagner, J. M., Qin, Q. P., Nguyen, T. H., Overgaard, M. T., Larsen, S. O., Sottrup-Jensen, L., Gleich, G. J. and Norgaard-Pedersen, B. (1999) The proform of eosinophil major basic protein: a new maternal serum marker for Down syndrome. Prenat. Diagn. **19**, 905–910

29 Sottrup-Jensen, L. (1995) A low-pH reverse-phase high-performance liquid chromatography system for analysis of the phenylthiohydantoins of S-carboxymethylcysteine and S-carboxyamidomethylcysteine. Anal. Biochem. **225**, 187–188
30 Grams, F., Dive, V., Yiotakis, A., Yiallouros, I., Vassiliou, S., Zwilling, R., Bode, W. and Stöcker, W. (1996) Structure of astacin with a transition-state analogue inhibitor. Nat. Struct. Biol. **3**, 671–675
31 Hangauer, D. G., Monzingo, A. F. and Matthews, B. W. (1984) An interactive computer graphics study of thermolysin-catalyzed peptide cleavage and inhibition by N-carboxymethyl dipeptides. Biochemistry **23**, 5730–5741
32 Matthews, B. W. (1988) Structural basis for the action of thermolysin and related zinc peptidases. Acc. Chem. Res. **21**, 333–340
33 Christianson, D. W. and Lipscomb, W. N. (1989) Carboxypeptidase A. Acc. Chem. Res. **22**, 62–69
34 Beaumont, A., O'Donohue, M. J., Paredes, N., Rousselet, N., Assicot, M., Bohuon, C., Fournie-Zaluski, M. C. and Roques, B. P. (1995) The role of histidine 231 in thermolysin-like enzymes. A site-directed mutagenesis study. J. Biol. Chem. **270**, 16803–16808
35 Mock, W. L. and Aksamawati, M. (1994) Binding to thermolysin of phenolate-containing inhibitors necessitates a revised mechanism of catalysis. Biochem. J. **302**, 57–68
36 Mock, W. L. and Yao, J. (1997) Kinetic characterization of the serralysins: a divergent catalytic mechanism pertaining to astacin-type metalloproteases. Biochemistry **36**, 4949–4958
37 Cha, J. and Auld, D. S. (1997) Site-directed mutagenesis of the active site glutamate in human matrilysin: investigation of its role in catalysis. Biochemistry **36**, 16019–16024
38 Jiang, W. and Bond, J. S. (1992) Families of metalloendopeptidases and their relationships. FEBS Lett. **312**, 110–114
39 Bode, W., Grams, F., Reinemer, P., Gomis-Rüth, F. X., Baumann, U., McKay, D. B. and Stöcker, W. (1996) The metzincin-superfamily of zinc-peptidases. Adv. Exp. Med. Biol. **389**, 1–11
40 Yiallouros, I., Grosse Berkhoff, E. and Stöcker, W. (2000) The roles of Glu93 and Tyr149 in astacin-like zinc peptidases. FEBS Lett. **484**, 224–228
41 Conover, C. A., Durham, S. K., Zapf, J., Masiarz, F. R. and Kiefer, M. C. (1995) Cleavage analysis of insulin-like growth factor (IGF)-dependent IGF-binding protein-4 proteolysis and expression of protease-resistant IGF-binding protein-4 mutants. J. Biol. Chem. **270**, 4395–4400
42 Byun, D., Mohan, S., Kim, C., Suh, K., Yoo, M., Lee, H., Baylink, D. J. and Qin, X. (2000) Studies on human pregnancy-induced insulin-like growth factor (IGF)-binding protein-4 proteases in serum: determination of IGF-II dependency and localization of cleavage site. J. Clin. Endocrinol. Metab. **85**, 373–381
43 Bergmann, U., Tuuttila, A., Stetler-Stevenson, W. G. and Tryggvason, K. (1995) Autolytic activation of recombinant human 72 kilodalton type IV collagenase. Biochemistry **34**, 2819–2825
44 Gilpin, B. J., Loechel, F., Mattei, M. G., Engvall, E., Albrechtsen, R. and Wewer, U. M. (1998) A novel, secreted form of human ADAM 12 (meltrin alpha) provokes myogenesis *in vivo*. J. Biol. Chem. **273**, 157–166

Received 28 March 2001/9 May 2001; accepted 15 June 2001